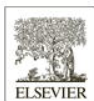


Provided for non-commercial research and education use.  
Not for reproduction, distribution or commercial use.



Volume 109      Number 7      May 2008      ISSN 0022-4073  
website: <http://www.elsevier.com/locate/jqsrt>

# Journal of Quantitative Spectroscopy & Radiative Transfer

Editors-in-Chief: M.P. Mengüç, M.I. Mishchenko and L.S. Rothman

This article was published in an Elsevier journal. The attached copy is furnished to the author for non-commercial research and education use, including for instruction at the author's institution, sharing with colleagues and providing to institution administration.

Other uses, including reproduction and distribution, or selling or licensing copies, or posting to personal, institutional or third party websites are prohibited.

In most cases authors are permitted to post their version of the article (e.g. in Word or Tex form) to their personal website or institutional repository. Authors requiring further information regarding Elsevier's archiving and manuscript policies are encouraged to visit:

<http://www.elsevier.com/copyright>



# On employing H<sub>2</sub><sup>16</sup>O, H<sub>2</sub><sup>17</sup>O, H<sub>2</sub><sup>18</sup>O, and D<sub>2</sub><sup>16</sup>O lines as frequency standards in the 15–170 cm<sup>-1</sup> window

Tibor Furtenbacher, Attila G. Császár\*

Laboratory of Molecular Spectroscopy, Institute of Chemistry, Eötvös University, P.O. Box 32, H-1518 Budapest 112, Hungary

Received 14 August 2007; received in revised form 1 October 2007; accepted 2 October 2007

## Abstract

The protocol MARVEL, standing for measured active rotational–vibrational energy levels, is used to study high-accuracy measurements of rotational lines of four isotopologues of water, H<sub>2</sub><sup>16</sup>O, H<sub>2</sub><sup>17</sup>O, H<sub>2</sub><sup>18</sup>O, and D<sub>2</sub><sup>16</sup>O, obtained by spectroscopy in the far-infrared (FIR) region of 15–170 cm<sup>-1</sup> by Matsushima et al. [Matsushima F, Odashima H, Iwasaki T, Tsunekawa S, Takagi K. Frequency measurement of pure rotational transitions of H<sub>2</sub>O from 0.5 to 5 THz. *J Mol Struct* 1995; 352/353, 371–8; Matsushima F, Nagase H, Nakauchi T, Odashima H, Takagi K. Frequency measurement of pure rotational transitions of H<sub>2</sub><sup>17</sup>O and H<sub>2</sub><sup>18</sup>O from 0.5 to 5 THz. *J Mol Spectrosc* 1999;193: 217–23; Matsushima F, Matsunaga M, Qian GY, Ohtaki Y, Wang RL, Takagi K. Frequency measurement of pure rotational transitions of D<sub>2</sub>O from 0.5 to 5 THz. *J Mol Spectrosc* 2001;206: 41–6; Matsushima F, Tomatsu N, Nagai T, Moriwaki Y, Takagi K. Frequency measurement of pure rotational transitions in the  $v_2 = 1$  state of H<sub>2</sub>O. *J Mol Spectrosc* 2006;235: 190–5]. MARVEL validates the high accuracy of most of the measured line positions. It results in a considerable number of energy levels with an average internal uncertainty of only 40 kHz ( $2\sigma$ ). It also supports serious inaccuracy problems when Watson-type *A*-reduced Hamiltonians are used for predicting the highly accurate rotational measurements for water. Finally, MARVEL suggests a large number of para-water levels, for example 41 for H<sub>2</sub><sup>16</sup>O, which are candidates for becoming frequency standards in the FIR region of 15–170 cm<sup>-1</sup> (the 0.5–5 THz window) when an accuracy of about 0.1 MHz is deemed to be sufficient.

© 2007 Elsevier Ltd. All rights reserved.

**Keywords:** MARVEL; Rotational spectra of water isotopologues; Rotational energy levels; Measurement standards

## 1. Introduction

An important feature of the best spectroscopic databases [1,2], achieved only in certain regions of the spectrum, is their internal consistency. Internal consistency means that, under the same experimental conditions, the observed wave numbers of the species can be reproduced, of course within the stated uncertainty, not only by repeated spectroscopic measurements but also by using the related energy levels determined by the measured transitions. Internal consistency of databases comprised by transitions (lines) and levels can be compromised in several ways; for example, by misassignments, misidentified reference lines, measurement errors (including calibration differences), or simple misprints. In order to help validation of

\*Corresponding author. Tel.: +36 137 22929; fax: +36 137 22592.

E-mail address: [csaszar@chem.elte.hu](mailto:csaszar@chem.elte.hu) (A.G. Császár).

assigned measurement results, spectroscopists developed several schemes, including effective Hamiltonian approaches [3], protocols based on (weighted) combination differences [4], and weighted least-squares methods [5–8]. We recently developed a new protocol and associated computer program MARVEL [9], standing for measured active rotational–vibrational energy levels. MARVEL can be used for determining rotational–vibrational energy levels from the observed transitions using an inversion method pioneered by Flaud et al. [5], and it results not only in uncertainties for the energy levels determined but also in improved uncertainty estimates for many of the observed lines. To achieve this, MARVEL builds also on the robust reweighting technique [10], which found several applications in spectroscopy [11,12], and on the Active Thermochemical Tables approach of Ruscic et al. [13]. If all of the observed wave numbers can be obtained from the MARVEL energy levels within their stated uncertainties, the levels and the transitions form a self-consistent set of data, and the related database is internally consistent.

In Ref. [9] we tested the MARVEL protocol and code on the example of the water isotopologue H<sub>2</sub><sup>17</sup>O and obtained accurate rotational–vibrational levels as well as improved uncertainty estimates for all the known experimental lines. An important finding was that MARVEL is well suited for checking the internal consistency of spectroscopic databases. In this study, MARVEL is used to check the internal accuracy and consistency of the mostly pure rotational transition measurements of Matsushima et al. [14–17] for the water isotopologues H<sub>2</sub><sup>16</sup>O, H<sub>2</sub><sup>17</sup>O, H<sub>2</sub><sup>18</sup>O, and D<sub>2</sub><sup>16</sup>O from 0.5 to 5 THz (about 15–170 cm<sup>−1</sup>). These measurements used a highly sensitive and accurate tunable far-infrared (FIR) spectrometer with an average accuracy of about 100–200 kHz, i.e., (3–6) × 10<sup>−6</sup> cm<sup>−1</sup> (1σ), somewhat worse than that of microwave and millimeter- and submillimeter wave spectrometers, which range from about 1 to about 50 kHz. The number of observed rotational transitions of Matsushima and co-workers, occasionally augmented by previous measurements, on the respective vibrational ground states of H<sub>2</sub><sup>16</sup>O, H<sub>2</sub><sup>17</sup>O, H<sub>2</sub><sup>18</sup>O, and D<sub>2</sub><sup>16</sup>O are 139, 127, 127, and 188, respectively. The number of observed rotational transitions in the  $v_2 = 1$  state of H<sub>2</sub><sup>16</sup>O, where  $v_2$  is the bending vibrational quantum number, is 130. As usual in high-resolution molecular spectroscopy, Matsushima et al. employed a Watson-type *A*-reduced Hamiltonian [3b] to obtain molecular parameters, which in turn governed the assignment of the measurements.

In the present work, we used MARVEL to check whether Matsushima's transitions contain considerable line-position errors preventing their use as frequency standards, an application suggested by Matsushima et al. [14–17] and investigated here in detail. The considerable precision of the measurements has been confirmed beyond reasonable doubt. This study also allows testing the accuracy of the effective *A*-reduced Watson Hamiltonian for a difficult case under the requirement of extreme accuracy. The scatter of the line frequencies produced by a Watson-type *A*-reduced Hamiltonian with up to 32 parameters can be substantial even for low rotational excitations. It seems that the related empirical data have an order of magnitude larger inaccuracy than the measured transitions themselves, therefore directly questioning the exclusive use of Watson-type Hamiltonians during such high-accuracy benchmark studies for more than the assignment of the lines. Furthermore, MARVEL allows deciding which of these lines can possibly be used as frequency standards in the 0.5–5 THz window. We suggest to consider those lines of H<sub>2</sub><sup>16</sup>O, H<sub>2</sub><sup>18</sup>O, and D<sub>2</sub><sup>16</sup>O as frequency standards, which have been measured with an internal precision of better than 33 kHz, whose underlying energy levels have been involved in at least three measured transitions in the FIR range, and which correspond to para-water. Next, the extremely accurate lines measured in the 0–0.5 THz window are compared with the predictions coming from the MARVEL energy levels determined from the lines measured [14–17] in the 0.5–15 THz window. These comparisons, available only for a very small number of transitions, mostly confirm the accuracy of the lines measured by Matsushima et al., though point out possible accuracy problems. Finally, the small number of transitions data allows the execution of a sensitivity analysis of the MARVEL energy levels, a task that is out of reach for much larger sets of experimental data, more typical of usual spectroscopic applications [9].

## 2. Methodological details

### 2.1. Determination of MARVEL energy levels

The relationship between the measured transitions,  $\sigma_i$ , and the experimental energy levels,  $E_{j_1(i)}$  and  $E_{j_2(i)}$ , is

$$\sigma_i = E_{j_1(i)} - E_{j_2(i)}. \quad (1)$$

Therefore, the MARVEL energy levels,  $\mathbf{X}$ , can be obtained by solving the generic matrix equation

$$\mathbf{AX} = \mathbf{B}, \quad (2)$$

where  $\mathbf{A} = \mathbf{a}^T \mathbf{g} \mathbf{a}$ ,  $\mathbf{B} = \mathbf{a}^T \mathbf{g} \mathbf{Y}$ ,  $g_i = 1/\delta_i^2$ , and  $\delta_i$  is the uncertainty assigned to the  $i$ th measured transition, the  $\mathbf{Y}$  vector contains the measured transitions, and the  $\mathbf{a}$  matrix is the design matrix that describes the relation between the transitions and the energy levels according to Eq. (1) (see Fig. 1 for a pictorial representation of the unweighted inversion protocol). Using the newly calculated energy levels one can determine the difference between the measured and computed transitions,

$$\Delta_i = \sigma_i - (E_{j_1(i)} - E_{j_2(i)}). \quad (3)$$

The  $\Delta_i$  values seem to provide an excellent gauge for the uncertainty of the measured transitions. If  $\Delta_i$  is much larger than the uncertainty of the  $i$ th measured transition,  $\delta_i$ , it indicates either a misassignment, a line position error, or an overly optimistic line uncertainty.

## 2.2. Adjustment of line uncertainties

In a previous publication [9], we found the robust reweighting technique, advocated by Lin et al. [11] and later by Watson [12] for spectroscopic applications, to be especially useful for adjustment of the uncertainties of the measured transitions. Within robust reweighting, one uses the simple adjustment formula

$$\tilde{g}_i = \frac{1}{\delta_i^2 + \alpha \Delta_i^2} \quad (4)$$

to increase the value of those uncertainties that cannot be reproduced well by the computed energy levels. In Eq. (4),  $\alpha$  is a positive number,  $\alpha \leq 1/3$  [12], chosen for the given spectroscopic database. Adjustment of the uncertainties is done in an iterative cycle, based on Eq. (4), which can be stopped when the quantity

$$\sum_i \frac{\tilde{g}_i \Delta_i^2}{N_t - N_\ell} \quad (5)$$

becomes as close to 1 as desired. In Eq. (5),  $N_t$  and  $N_\ell$  denote the number of transitions and the number of energy levels, respectively.

While the robust reweighting technique works very well in case of overly optimistic uncertainties, leading to systematic increases of line uncertainties, a disadvantage of robust fitting is that one is not allowed to *reduce* the value of the uncertainties. Nevertheless, as turned out in this study, this might become necessary in those cases when the given uncertainties are too pessimistic. One way forward is that one can reduce the values of the uncertainties artificially, and start the robust fitting procedure with these reduced uncertainties. If the value

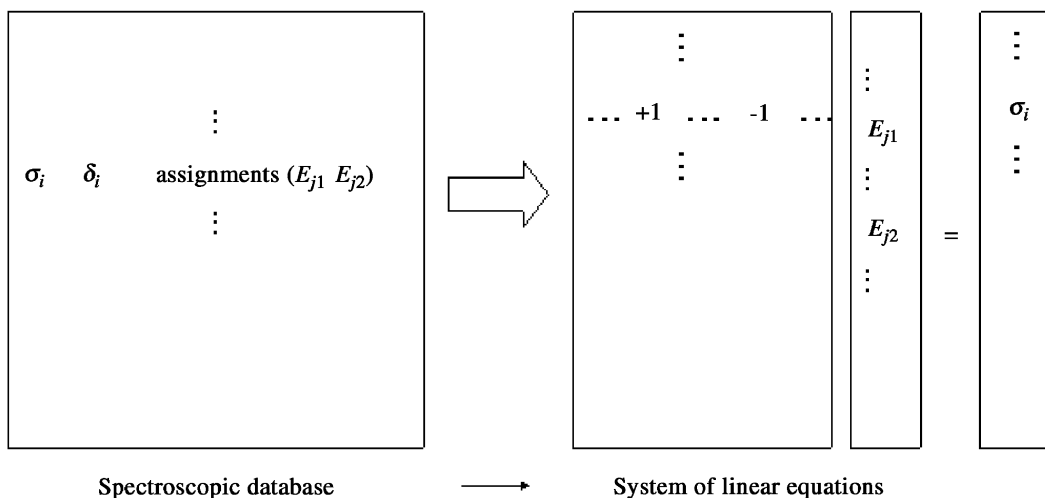


Fig. 1. Pictorial representation of the MARVEL approach for the inversion of experimental line information to derive energy levels.

of a reduced uncertainty does not change during robust fitting, and enough data are available, it indicates that the original uncertainty was too pessimistic.

### 2.3. Uncertainties of levels

After executing the robust reweighting procedure, one obtains a self-consistent database, in which each transition can be reproduced by the MARVEL energy levels. In a self-consistent database, the uncertainties of the experimental energy levels can simply be computed as [9,13]

$$\varepsilon_j = t \sqrt{A_{jj}^{-1}}. \quad (6)$$

For  $t = 2$ ,  $\varepsilon_j$  represents a  $\sim 95\%$  confidence limit for the uncertainty of the levels.

### 2.4. Sensitivity analysis

Sometimes it is useful to know those transitions that influence the uncertainty of a given experimental energy level. This information can be obtained via the computation of the sensitivity matrix  $\mathbf{S}$ . We computed the elements of the  $\mathbf{S}$  matrix both numerically and analytically. The numerical calculation is based on the well-known Gauss-type error propagation. The analytical expression, employed in MARVEL, for the sensitivity matrix calculation was [13]

$$S_{ji} = \frac{\partial E_j}{\partial T_i} = \sum_k^{N_\ell-1} \frac{A_{jk}^{-1} a_{ik}}{\delta_i^2}. \quad (7)$$

The absolute values of the elements of  $\mathbf{S}$  are between 0 and 1. The larger the value of an element of the sensitivity matrix, the larger the influence of the transitions on the given energy level.

## 3. Results and discussion

### 3.1. MARVEL energy levels

For all symmetrically substituted isotopologues of water, the observed transitions can be divided unequivocally into two main spectroscopic networks (SNs), para (SN1) and ortho (SN2) [18]. Those energy levels belong to the para SN for which the number ( $K_a + K_c + v_3$ ) is even, where  $K_a$  and  $K_c$  come from the standard rotation notation ( $J_{K_a K_c}$ ) and  $v_3$  is the vibrational quantum number corresponding to the antisymmetric stretching in the standard normal coordinate labeling ( $v_1 v_2 v_3$ ) of water.

Tables 1 and 2 show the computed SN1 (para) and SN2 (ortho) MARVEL energy levels and the associated uncertainties (in  $\text{cm}^{-1}$ ) of the isotopologues  $\text{H}_2^{16}\text{O}$ ,  $\text{H}_2^{17}\text{O}$ ,  $\text{H}_2^{18}\text{O}$ ,  $\text{D}_2^{16}\text{O}$ , and  $\text{H}_2^{16}\text{O}$  ( $v_3 = 1$  state). Due to the appropriate selection rules, transitions between the energy levels of SN1 and SN2 cannot be measured directly. Therefore, the lowest SN2 level must be estimated from empirical and/or theoretical considerations. The first row of Table 2, corresponding to the rotational  $1_{01}$  energy levels, represents the ‘magic numbers’ used in this study to connect the two SNs. These ‘magic numbers’ were taken from Ref. [19]. Fortunately, any inaccuracy in these numbers will not affect the accuracy of transitions based on the MARVEL levels. Both the computed energy levels and their uncertainties, reported in Tables 1 and 2, were determined using the original uncertainties of the measured transitions, taken from Refs. [14–17]. We used  $\alpha = 0.01$  for executing the robust reweighting procedure, allowing for a very slow and delicate adjustment of the line position uncertainties. Note, finally, that the small splittings in the *ortho*-water lines, on the order of 20–30 kHz, are not taken into account during the present analysis as there are only very few instances where these have been resolved. Nevertheless, only the *para*-water lines will be considered as frequency standards.

The uncertainties of most of the energy levels is only  $1\text{--}2 \times 10^{-6} \text{ cm}^{-1}$  ( $2\sigma$ ), corresponding to a few tens of kHz uncertainties for the related transitions. These numbers are in full accord with the expected uncertainties

Table 1

Pure rotational SN1 (para) MARVEL energy levels and associated uncertainties (all in  $\text{cm}^{-1}$ ) of four water isotopologues based on experimental transitions measured by Matsushima et al. [14–17] between 0.5 and 5 THz

$J$	$K_a$	$K_c$	$\text{H}_2^{16}\text{O}$	$\text{H}_2^{17}\text{O}$	$\text{H}_2^{18}\text{O}$	$\text{D}_2^{16}\text{O}$	$\text{H}_2^{16}\text{O } v_2 = 1$
0	0	0	0.000000(0)	0.000000(0)	0.000000(0)	0.000000(0)	0.000000(0)
1	1	1	37.1371186(3)	36.9311103(7)	36.7486524(7)	20.2589938(7)	40.2207806(47)
2	0	2	70.0908033(4)	70.0046402(10)	69.9274140(9)	35.8780167(8)	70.2182653(50)
2	1	1	95.1759243(4)	94.9705340(11)	94.7886146(10)	49.3393906(10)	98.9036200(55)
2	2	0	136.1639004(4)	135.4311641(10)	134.7830792(9)	74.1419968(9)	148.7400141(48)
3	1	3	142.2784654(5)	141.9023831(10)	141.5680226(9)	74.5062294(9)	144.7373819(50)
3	2	2	206.3013987(5)	205.4817665(11)	204.7558212(10)	110.0340344(10)	219.0412591(50)
3	3	1	285.2193043(6)	283.5615484(13)	282.0944411(11)	156.6054302(10)	312.7050656(63)
4	0	4	222.0527303(5)	221.6207967(12)	221.2339604(11)	114.9865133(10)	222.7048511(50)
4	1	3	275.4970025(5)	275.1304942(12)	274.8031328(11)	141.0869296(10)	280.7233683(52)
4	2	2	315.7794885(6)	315.0784540(13)	314.4593818(11)	164.1776878(10)	328.1547630(54)
4	3	1	383.8424592(7)	382.1758553(13)	380.7023655(12)	206.2764876(11)	411.1706728(61)
4	4	0	488.1340965(7)	485.2367021(15)	482.6724636(13)	269.3811286(11)	534.8722713(61)
5	1	5	326.6254226(8)	325.8801340(13)	325.2156602(11)	170.2429871(11)	328.0827139(54)
5	2	4	416.2086827(8)	415.1279766(13)	414.1680632(12)	217.5854800(11)	429.4062857(55)
5	3	3	503.9680336(9)	502.1795367(15)	500.5961121(13)	267.5304344(11)	531.6613436(58)
5	4	2	610.1143465(9)	607.1591234(16)	604.5440280(14)	331.0717861(11)	656.9489150(68)
5	5	1		737.6202539(19)	733.6791419(15)	411.5414997(12)	811.3944913(75)
6	0	6	446.6965278(9)	445.7191443(14)	444.8461063(13)	232.5217378(12)	447.0341622(66)
6	1	5	542.9057035(9)	541.9966777(15)	541.1800298(14)	279.5646683(12)	551.5173486(65)
6	2	4	602.7734104(9)	601.9607090(16)	601.2376831(13)	309.2650843(12)	616.4442454(63)
6	3	3	661.5488229(10)	659.9865764(16)	658.6099323(14)	345.4467028(12)	687.8432099(65)
6	4	2	757.7800839(10)	754.8115271(17)	752.1872691(15)	405.5316362(12)	804.4190543(72)
6	5	1	888.6325281(15)	884.1134644(19)	880.1143493(18)	485.5997608(12)	958.1333224(73)
6	6	0	1045.0581962(18)	1038.7649924(45)	1033.1942719(25)	582.4084659(14)	1139.2165132(74)
7	1	7	586.4791021(17)	585.1617759(16)	583.9863518(14)	305.7668077(13)	586.3434889(75)
7	2	6	709.6081163(11)	708.0161834(16)	706.5976563(14)	369.2660877(12)	723.7935130(67)
7	3	5	816.6941242(11)	814.6104662(17)	812.7615090(15)	427.1986319(12)	845.2080688(69)
7	4	4	927.7437746(13)	924.6412288(18)	921.8955915(16)	492.0215172(12)	974.7615729(70)
7	5	3		1055.0537449(23)	1050.9899877(18)	572.1302364(13)	1129.2950140(72)
7	6	2		1209.8129473(27)	1204.1690833(116)	668.8513582(14)	
7	7	1				781.1716825(15)	
8	0	8	744.0635572(18)	742.3984393(42)	740.9121484(15)	388.0186591(13)	742.7168773(85)
8	1	7	882.8902059(20)	881.0987827(17)	879.4946350(16)	457.8229448(13)	895.6076917(75)
8	2	6	982.9115782(20)	981.4957012(18)	980.2221060(17)	505.0487239(13)	1001.0664998(71)
8	3	5	1050.1575177(20)	1048.6567220(21)	1047.3283935(18)	540.8815062(13)	1076.0432382(71)
8	4	4	1131.7754116(20)	1128.9378205(22)		593.5866529(13)	1176.9436788(72)
8	5	3	1255.9113655(20)	1251.2907036(24)		671.3354662(14)	
8	6	2	1411.6416887(21)	1405.1805102(127)		767.7206578(16)	
8	7	1		1582.1966060(128)		880.0545391(19)	
9	1	9	920.2098637(23)	918.1402799(43)			
9	2	8	1080.3852849(22)	1078.0201095(45)			1095.8472192(73)
9	3	7	1216.2310871(21)	1213.5619690(46)			1246.6843444(76)
9	4	6	1340.8846902(21)				1388.5766050(76)
9	5	5	1474.9805778(24)				1544.7293216(83)
9	6	4	1631.2452561(28)			879.0278790(20)	

of the measured levels. Interestingly, by far the most precise measurements have been performed for  $\text{D}_2^{16}\text{O}$ . For all four isotopologues, except  $\text{H}_2^{16}\text{O}$ , where the  $5_{51}$  and  $5_{50}$  rotational levels on the ground vibrational state are missing, a complete set of rotational levels is available for  $J = 1, 2, 3, 4, 5$ , and 6. Further, more or less complete sets of rotational levels are available for up to  $J = 11$ . It is recommended that these levels should be used when comparison of first-principles theoretical predictions to experimental results [20] is needed in this region or when these energy levels are used as lower states to make new assignments.

Table 2

Pure rotational SN2 (ortho) MARVEL energy levels and the associated uncertainties (all in  $\text{cm}^{-1}$ ) of water isotopologues based on experimental transitions measured by Matsushima et al. [14–17] between 0.5 and 5 THz

$J K_a K_c$	$\text{H}_2^{16}\text{O}$	$\text{H}_2^{17}\text{O}$	$\text{H}_2^{18}\text{O}$	$\text{D}_2^{16}\text{O}$	$\text{H}_2^{16}\text{O } v_2 = 1$
1 0 1 <sup>a</sup>	23.7943500(0)	23.7735100(0)	23.7549020(0)	12.11170200(0)	23.8108600(0)
1 1 0	42.3717266(2)	42.1869508(10)	42.0234183(5)	22.6843232(5)	45.7595813(32)
2 1 2	79.4963699(4)	79.2273357(9)	78.9886385(6)	42.0693065(6)	82.3151878(32)
2 2 1	134.9016127(4)	134.1452588(10)	133.4757478(6)	73.6763837(6)	147.5593795(32)
3 0 3	136.7616330(4)	136.5375976(11)	136.3366288(7)	70.4475232(7)	137.1504251(33)
3 1 2	173.3657775(4)	173.1100665(11)	172.8828709(8)	88.9713436(7)	177.6671846(32)
3 2 1	212.1563272(5)	211.4357406(12)	210.7991960(8)	112.2515376(7)	224.5888315(32)
3 3 0	285.4185251(5)	283.7676998(11)	282.3069621(8)	156.6628384(8)	312.8694656(33)
4 1 4	224.8383471(6)	224.3041956(13)	223.8284663(8)	117.3120508(8)	226.8505272(33)
4 2 3	300.3622366(9)	299.4388679(13)	298.6200542(8)	158.1109916(8)	313.2700373(33)
4 3 2	382.5168272(9)	380.8057991(14)	379.2914865(9)	205.8862444(8)	410.0693753(38)
4 4 1	488.1076186(12)	485.2088769(16)	482.6433840(11)	269.3752266(9)	534.8528739(39)
5 0 5	325.3478526(9)	324.6609104(14)	324.0466780(9)	169.0385174(9)	326.0202422(37)
5 1 4	399.4574526(9)	398.8792651(14)	398.3604229(10)	204.9375649(8)	406.1167193(38)
5 2 3	446.5106001(9)	445.7933459(14)	445.1584854(10)	229.9919157(8)	459.2223782(39)
5 3 2	508.8119783(9)	507.1742205(16)	505.7286636(10)	269.0100700(9)	535.7479688(39)
5 4 1	610.3410739(10)	607.3972277(18)	604.7927223(12)	331.1235058(9)	657.1161683(42)
5 5 0		737.6237454(34)	733.6828390(13)	411.5420532(10)	811.3967129(42)
6 1 6	447.2522793(9)	446.2448418(14)	445.3461208(10)	233.1057424(9)	448.0070234(40)
6 2 5	552.9113070(9)	551.6092663(15)	550.4507152(11)	288.0937633(9)	566.5397064(40)
6 3 4	648.9785894(11)	647.0719651(16)	645.3824490(11)	341.3887117(9)	676.9658893(41)
6 4 3	756.7246641(11)	753.7048267(18)	751.0327517(13)	405.2832856(9)	803.6351183(53)
6 5 2	888.5986065(12)	884.0773210(20)	880.0760476(14)	485.5938327(9)	958.1108756(53)
6 6 1	1045.0577882(14)	1038.7645882(23)	1033.1938022(125)	582.4084148(11)	1139.2163198(58)
7 0 7	586.2434539(10)	584.9407731(17)	583.7777180(12)	305.4949584(10)	585.8965797(41)
7 1 6	704.2139436(10)	702.8857127(17)	701.6941171(12)	364.0467459(9)	714.9838566(40)
7 2 5	782.4097075(11)	781.3772010(17)	780.4526724(13)	401.2622982(10)	797.8462001(41)
7 3 4	842.3564637(11)	840.8646109(18)	839.5492863(13)	436.0601238(10)	868.1289189(49)
7 4 3	931.2369629(12)	928.2956564(19)	925.6995494(14)	492.8802891(10)	977.3927940(50)
7 5 2	1059.8352841(14)		1051.2028959(18)	572.1644121(11)	1129.4207298(55)
7 6 1	1216.1943172(15)		1204.1745837(28)	668.8519915(12)	1310.6871108(55)
7 7 0			1378.9859931(30)	781.1716945(14)	
8 1 8	744.1625535(13)	742.4905545(19)	740.9984846(20)	388.1421303(10)	742.9204315(43)
8 2 7	885.6000749(12)	883.6517644(19)	881.9139186(14)	460.7655054(10)	900.4194901(51)
8 3 6	1006.1157850(12)	1003.7809800(20)	1001.7055500(18)	524.6087049(11)	1035.4462187(51)
8 4 5	1122.7083654(14)	1119.4877425(21)	1116.6359170(19)	591.2182598(11)	1169.9510473(51)
8 5 4	1255.1665628(15)		1246.3682683(20)	671.1949666(12)	1324.8865718(52)
8 6 3	1411.6112298(17)		1399.4276547(34)	767.7164756(14)	
8 7 2				880.0544813(16)	
9 0 9	920.1682076(25)	918.1018078(21)	916.2575168(48)		
9 1 8	1079.0794168(16)	1076.8006697(22)	1074.7627850(33)		1093.3335254(59)
9 2 7	1201.9213193(15)	1199.9627384(25)	1198.1993660(28)		1223.6516792(58)
9 3 6	1282.9189163(15)	1281.2681408(22)	1279.7973447(27)		1309.9240240(55)
9 4 5	1360.2351320(15)	1357.5553891(24)			1404.0199219(53)
9 5 4	1477.2971429(21)	1472.6844192(82)			1546.2995762(56)
9 6 3	1631.3827657(22)	1624.8417027(82)		879.0477020(16)	
9 7 2		1801.9895949(87)			
10 2 9	1293.6338237(23)				
10 3 8	1446.1279993(23)				
10 4 7	1581.3357201(22)				
10 5 6	1718.7185333(24)				
10 6 5	1874.9726793(24)				
11 2 9	1690.6641043(30)				
11 3 8	1813.2231075(28)				
11 4 7	1899.0078629(28)				
11 5 6	1998.9949927(26)				
11 6 5	2144.0459250(32)				

<sup>a</sup>The  $1_{01}$  ‘magic numbers’ (see text) were taken from Ref. [19].

### 3.2. Measured frequencies with improved uncertainties

Tables 3–7 show the measured transitions with the original experimental uncertainties. These tables reveal how the *A*-reduced Watsonian, used by Matsushima et al. [14–17], and how MARVEL reproduce the measured transitions. The MARVEL transitions reported were calculated after executing a robust fitting, with  $\alpha = 0.01$ , and uncertainties of the MARVEL transitions, given in parentheses, were computed using the uncertainties of the two energy levels taking part in the given transition and using Gauss-type error propagation. Contributions to the uncertainties of the measured line positions include the uncertainty of the synthesized FIR frequency and that of the determination of the center frequency of the spectral line. Overall, in most cases the typical estimated uncertainty of the measurements of Matsushima and co-workers [14–17] is about 100 kHz ( $2\sigma$ ). In a few cases Matsushima et al. indicated large uncertainties for the measured transitions. For example, for the  $4_{23} \leftarrow 3_{30}$  line of  $\text{H}_2^{17}\text{O}$  they indicated an unusually large uncertainty of 702 kHz ( $2\sigma$ ), as a result of the unresolved hyperfine splitting due to the quadrupole moment of  $^{17}\text{O}$ . This estimate is confirmed here by an unusually large observed–calculated (O–C) value of 525 kHz ( $2\sigma$ ).

In Tables 3–7 the entries given in bold face are the wave numbers suggested to be dependable measurement standards by MARVEL. Due to the hyperfine splitting mentioned above, the  $\text{H}_2^{17}\text{O}$  lines have not been considered in this study as desirable frequency standards. The selection process for  $\text{H}_2^{16}\text{O}$ ,  $\text{H}_2^{18}\text{O}$ , and  $\text{D}_2^{16}\text{O}$  is based on (a) the small uncertainty of the measured transition confirmed by MARVEL, the MARVEL O–C value should be less than 33 kHz ( $1 \times 10^{-6} \text{ cm}^{-1}$ ); (b) the fact that both energy levels involved in the transition take part in at least two more transitions, helping to fix the energy levels; and (c) transitions corresponding to *para*-water. It is clear that a considerable number of observed transitions of the  $\text{H}_2^{16}\text{O}$ ,  $\text{H}_2^{18}\text{O}$ , and  $\text{D}_2^{16}\text{O}$  isotopologues could serve as frequency standards in the 15–170  $\text{cm}^{-1}$  window. A further test on the accuracy of the measured lines is given in Section 3.4 (vide infra).

The results found in these tables and especially on the related Fig. 2 show that the MARVEL procedure can reproduce the measured transitions significantly better than the *A*-reduced Watsonian. The water molecule is known to show an extremely large centrifugal distortion effect and thus effective Hamiltonians of the Watson form are expected to display unusually large errors for highly excited rotational levels (see, e.g., Ref. [21]). This expectation is confirmed in this study with the additional result that the Watson *A*-reduced Hamiltonian performs relatively poorly even for low rotational excitations and unable to result in precise energy values approaching that of the measurements of Matsushima et al. Watson's *A*-reduced Hamiltonian is unable to reproduce the measured transitions to be better than 1000 kHz. As clearly seen in Fig. 2, for  $\text{H}_2^{16}\text{O}$  there are three transitions that have errors considerably larger than 1000 kHz. In contrast, MARVEL reproduces almost all measured rotational levels with an average uncertainty better than 40 kHz.

As mentioned in Section 2.3, robust reweighting cannot be used for the *reduction* of experimental uncertainties. Therefore, we decided to reduce the uncertainties of the lines artificially. Using these reduced uncertainty values we restarted the robust reweighting procedure and checked which reduced uncertainties increased during the iterative procedure. Those original uncertainties that did not increase during robust fitting were too pessimistic, suggesting that one can use smaller uncertainties. Increase in an uncertainty during the fitting cycles indicates that uncertainty of this line was too optimistic; therefore, a larger value should be used. The initial uncertainty values for these robust fitting tests were 1/2, 1/4, 1/10, and 1/20 of the original experimental uncertainties. The adjusted values are usually smaller than those assigned to the lines by Matsushima et al., confirming the high overall precision of the measurements. In the case of this small dataset obtained under the same experimental conditions, the increased uncertainties, whether the correction factor was 1/2, 1/4, 1/10, or 1/20, always belonged to the same transitions, suggesting the validity of this approach. The improved uncertainties of the measured transitions can be found in the Supplementary Material.

### 3.3. Sensitivities of levels on lines

Table 8 shows the computed sensitivity matrix  $\mathbf{S}$  for selected SN1 energy levels of the  $\text{H}_2^{16}\text{O}$  isotopologue. The table contains only those elements of the  $\mathbf{S}$  matrix that are larger than 0.25. The numbers in parentheses show the serial number, taken from Table 3, of the transition that has the given effect on the energy level. According to Table 8, the most important transitions are  $0_{00} \rightarrow 1_{11}$  (serial number: 7) and  $1_{11} \rightarrow 2_{02}$

Table 3

Measured and calculated H<sub>2</sub><sup>16</sup>O transitions<sup>a</sup>

No.	Frequency (MHz)	Obs–Calc. (kHz)		No.	Frequency (MHz)	Obs–Calc. (kHz)	
		Watsonian	MARVEL			Watsonian	MARVEL
1	556,935.819(13)	222	1(1)	71	3,126,585.070(13)	-419	0(3)
2	<b>752,033.104(13)</b>	<b>251</b>	<b>-11(2)</b>	72	3,135,010.951(16)	410	68(3)
3	<b>916,171.405(13)</b>	<b>-592</b>	<b>3(2)</b>	73	3,149,876.898(33)	206	-4(6)
4	970,314.968(18)	37	-141(3)	74	3,165,532.734(46)	-353	0(5)
5	<b>987,926.743(16)</b>	<b>-373</b>	<b>-7(1)</b>	75	3,167,578.237(23)	-155	-169(4)
6	1,097,364.791(13)	127	-7(2)	76	3,182,186.848(13)	-76	-2(4)
7	1,113,342.964(16)	472	0(1)	77	<b>3,210,358.196(13)</b>	<b>353</b>	<b>-6(4)</b>
8	1,153,126.822(13)	150	10(2)	78	3,230,146.525(20)	-47	15(5)
9	1,158,323.743(25)	31	8(4)	79	3,245,323.573(40)	809	FSN1
10	1,162,911.593(13)	-404	5(2)	80	3,307,402.532(84)	-531	FSN2
11	<b>1,207,638.714(13)</b>	<b>-514</b>	<b>-4(2)</b>	81	3,329,185.239(40)	-229	5(12)
12	<b>1,228,788.772(13)</b>	<b>-83</b>	<b>-11(2)</b>	<b>82</b>	<b>3,331,458.376(18)</b>	<b>-89</b>	<b>-4(2)</b>
13	1,278,265.946(20)	45	0(5)	83	3,495,358.110(36)	-517	-6(6)
14	1,296,411.033(13)	-381	1(5)	84	3,509,431.278(37)	228	-13(8)
15	1,322,064.803(13)	244	3(4)	85	3,536,666.807(23)	-180	3(4)
16	1,410,618.074(13)	-396	0(4)	86	3,599,641.708(44)	-499	28(4)
17	<b>1,440,781.544(27)</b>	<b>-252</b>	<b>-28(4)</b>	87	3,612,970.623(71)	395	23(5)
18	1,541,966.785(23)	35	-242(4)	88	3,654,603.282(18)	173	-1(4)
19	<b>1,602,219.182(16)</b>	<b>217</b>	<b>-15(2)</b>	89	3,669,872.251(100)	-236	44(7)
20	1,661,007.637(22)	-357	12(2)	90	3,674,226.995(65)	1504	0(12)
21	1,669,904.775(37)	543	-5(1)	91	3,682,708.105(38)	-103	0(7)
22	1,713,882.973(13)	29	-8(4)	92	3,691,315.309(91)	-718	-189(6)
23	1,716,769.633(13)	-369	-5(2)	93	3,718,095.940(56)	368	0(11)
24	1,762,042.791(13)	162	6(4)	94	3,721,502.796(18)	-223	0(9)
25	<b>1,766,198.748(13)</b>	<b>111</b>	<b>7(4)</b>	95	3,737,021.532(22)	-411	0(9)
26	<b>1,794,788.953(13)</b>	<b>-249</b>	<b>2(4)</b>	<b>96</b>	<b>3,798,281.638(44)</b>	<b>141</b>	<b>-21(4)</b>
27	1,797,158.762(16)	284	-28(5)	97	3,807,258.412(22)	-321	-186(3)
28	1,867,748.594(13)	8	4(4)	98	3,855,281.595(89)	126	372(6)
29	1,884,887.822(18)	-523	1(6)	99	3,922,858.136(62)	369	0(6)
30	1,918,485.324(16)	-88	6(4)	100	3,970,997.405(54)	-307	-11(6)
31	<b>1,919,359.531(13)</b>	<b>-402</b>	<b>8(2)</b>	101	3,977,046.481(84)	-182	456(2)
32	2,015,982.828(32)	94	-4(8)	102	4,000,164.750(71)	-183	-97(5)
33	2,040,476.810(20)	153	-2(3)	103	4,020,094.138(62)	-825	-0(10)
34	<b>2,074,432.305(16)</b>	<b>271</b>	<b>0(2)</b>	104	4,053,426.066(25)	101	2(10)
35	2,164,131.980(18)	595	9(2)	105	4,072,555.267(47)	453	0(9)
36	2,196,345.756(16)	447	11(2)	106	4,118,633.703(44)	-1026	0(10)
37	2,221,750.500(18)	614	275(4)	107	4,161,918.741(120)	-1000	-68(8)
38	2,244,810.924(20)	-262	-4(5)	108	4,166,851.176(28)	-81	6(4)
39	2,264,149.650(13)	-352	85(3)	109	4,190,576.643(62)	513	-100(6)
40	2,317,882.160(16)	-1	1(6)	<b>110</b>	<b>4,218,430.618(40)</b>	<b>-198</b>	<b>-21(3)</b>
41	2,344,250.335(18)	-164	-20(4)	111	4,240,191.823(37)	-560	932(5)
42	2,347,482.172(32)	-871	FSN1	112	4,279,695.925(65)	-139	FSN1
43	2,365,899.659(20)	394	37(2)	113	4,345,505.100(50)	-371	FSN1
44	<b>2,391,572.628(13)</b>	<b>-375</b>	<b>-3(2)</b>	114	4,348,518.162(97)	-1527	0(12)
45	2,428,247.209(16)	-317	0(6)	115	4,366,791.768(84)	-1198	ORP2
46	<b>2,446,843.245(20)</b>	<b>368</b>	<b>0(8)</b>	116	4,435,759.411(36)	1178	FSN1
47	2,462,933.032(13)	-34	23(4)	117	4,456,621.984(44)	13	-147(2)
48	2,477,452.945(69)	10	FSN2	118	4,468,569.050(23)	176	-169(2)
49	<b>2,531,917.811(23)</b>	<b>3</b>	<b>0(9)</b>	119	4,512,384.121(30)	143	-24(2)
50	2,567,177.132(13)	293	5(5)	120	4,519,563.921(25)	25	FSN1
51	2,571,762.630(13)	-175	0(12)	121	4,535,939.553(20)	-300	-15(4)
52	2,575,004.634(44)	618	893(8)	122	4,571,661.011(25)	-318	0(10)
53	<b>2,630,959.520(27)</b>	<b>-134</b>	<b>0(4)</b>	123	4,600,431.452(25)	-163	-13(4)
54	2,640,473.836(16)	442	4(2)	124	4,619,371.406(22)	-924	0(9)
55	2,664,570.704(16)	248	-1(5)	125	4,668,678.294(37)	-501	0(9)

Table 3 (continued)

No.	Frequency (MHz)	Obs–Calc. (kHz)		No.	Frequency (MHz)	Obs–Calc. (kHz)	
		Watsonian	MARVEL			Watsonian	MARVEL
56	2,685,638.969(18)	−271	17(3)	126	4,684,382.106(34)	1294	0(10)
57	2,773,976.588(20)	−41	1(1)	127	4,684,697.855(77)	318	0(11)
58	2,848,996.260(100)	123	ORP1	128	4,687,526.543(30)	455	0(6)
59	2,880,025.369(30)	−50	293(4)	129	4,689,524.212(50)	−360	0(7)
<b>60</b>	<b>2,884,278.940(18)</b>	<b>410</b>	<b>8(4)</b>	130	4,690,093.784(42)	91	0(7)
<b>61</b>	<b>2,884,941.052(18)</b>	<b>50</b>	<b>19(4)</b>	131	4,690,528.924(40)	−180	0(6)
62	2,962,111.094(16)	48	3(4)	132	4,693,044.499(56)	923	ORP3
<b>63</b>	<b>2,968,748.654(16)</b>	<b>−171</b>	<b>7(1)</b>	133	4,724,263.773(23)	134	−2(7)
64	2,970,800.244(16)	236	−9(4)	134	4,734,296.171(25)	1175	3(5)
65	2,997,539.160(47)	−34	0(12)	135	4,764,038.870(104)	774	0(9)
66	2,998,565.722(22)	11	−2(9)	136	4,801,938.995(28)	716	0(10)
67	3,003,347.566(41)	280	−18(4)	137	4,802,992.161(23)	−82	2(6)
68	3,013,199.566(23)	−558	−27(3)	138	4,850,334.680(37)	−170	−47(3)
69	3,043,766.149(25)	−116	8(4)	139	4,869,963.371(59)	−688	FSN2
70	3,118,998.512(25)	−419	−2(9)				

<sup>a</sup>FSN = floating spectroscopic network, ORP = orphan (see Ref. [9] and the text for more details). Recommended frequency standards are indicated in bold face.

Table 4  
Measured and calculated H<sub>2</sub><sup>17</sup>O transitions<sup>a</sup>

No.	Frequency (MHz)	Obs–Calc. (kHz)		No.	Frequency (MHz)	Obs–Calc. (kHz)	
		Watsonian	MARVEL			Watsonian	MARVEL
1	13,535.510(10)	51	−1(6)	66	3,158,746.404(36)	−53	−17(6)
2	194,002.290(10)	50	−2(4)	67	3,195,616.643(38)	116	−11(7)
3	469,809.339(351)	−589	−525(5)	68	3,196,773.182(36)	−67	−34(7)
4	552,021.075(38)	10	−70(3)	69	3,298,639.736(56)	44	−4(7)
5	658,504.180(149)	−360	−348(7)	70	3,313,043.876(46)	−178	7(5)
6	748,458.779(42)	162	10(4)	71	3,451,481.974(428)	55	0(26)
7	944,853.071(42)	−20	−120(5)	72	3,468,801.961(38)	1915	0(9)
8	987,879.876(39)	−151	−5(6)	73	3,535,900.842(39)	427	13(7)
9	991,519.683(36)	4	59(4)	74	3,592,683.645(39)	−269	−6(6)
10	1,096,415.186(36)	110	−5(5)	75	3,601,383.801(51)	−45	14(8)
11	1,107,166.987(36)	91	0(2)	76	3,644,995.072(39)	63	−4(6)
12	1,148,974.962(36)	23	−2(5)	77	3,668,047.672(60)	137	0(10)
13	1,168,135.700(36)	9	−12(4)	78	3,683,082.986(39)	46	−10(7)
14	1,189,418.871(38)	44	0(7)	79	3,787,242.695(44)	−154	−22(5)
15	1,197,609.827(36)	123	−47(5)	80	3,803,428.532(77)	−74	23(6)
16	1,212,979.348(36)	−86	3(4)	81	3,876,375.114(85)	75	9(8)
17	1,214,991.983(51)	218	3(8)	82	3,904,093.332(156)	22	0(1)
18	1,282,726.792(42)	16	21(8)	83	3,908,469.423(53)	−52	−178(8)
19	1,325,632.503(38)	−61	−28(8)	84	3,909,669.422(80)	−509	0(9)
20	1,332,129.386(38)	117	39(7)	85	3,911,126.846(60)	199	0(7)
21	1,406,448.955(38)	147	0(6)	86	4,026,370.245(48)	50	1(7)
22	1,439,891.568(149)	32	−26(7)	87	4,036,624.943(46)	333	FSN3
23	1,583,727.403(38)	−112	−17(7)	88	4,063,443.292(56)	−115	0(19)
24	1,604,180.557(38)	−33	−40(5)	89	4,082,007.509(64)	−155	FSN3
25	1,646,398.143(39)	14	−2(4)	90	4,158,000.015(77)	−173	18(7)
26	1,662,464.158(36)	64	53(3)	91	4,180,385.495(48)	−147	−16(6)
27	1,718,118.736(38)	−7	70(4)	92	4,197,019.729(42)	180	205(5)
28	1,739,572.000(36)	52	15(7)	93	4,231,907.193(39)	−77	−7(8)
29	1,783,388.025(36)	−52	92(7)	94	4,351,161.455(48)	−358	ORP
30	1,840,152.668(36)	21	83(6)	95	4,413,848.064(42)	66	20(5)

Table 4 (continued)

No.	Frequency (MHz)	Obs–Calc. (kHz)		No.	Frequency (MHz)	Obs–Calc. (kHz)	
		Watsonian	MARVEL			Watsonian	MARVEL
31	1,906,062.231(36)	−149	−1(5)	96	4,440,837.832(80)	30	6(5)
32	1,948,277.941(36)	145	28(6)	97	4,485,568.539(44)	−73	−26(5)
33	2,011,529.712(36)	−106	−57(5)	98	4,535,154.497(56)	352	92(7)
34	2,013,437.033(51)	−484	0(8)	99	4,561,561.243(53)	473	0(3)
35	2,088,016.649(36)	80	31(5)	100	4,564,109.765(39)	156	FSN3
36	2,155,440.437(36)	146	31(4)	101	4,613,500.984(680)	−1626	0(3)
37	2,168,457.888(38)	−94	−1(5)	102	4,630,833.514(816)	2090	ORP
38	2,225,010.637(39)	−105	27(6)	103	4,578,730.854(60)	130	−33(6)
39	2,252,481.128(36)	−199	3(5)	104	4,633,687.667(123)	993	FSN1
40	2,262,993.376(46)	−230	−11(8)	105	4,636,270.403(71)	−1265	FSN2
41	2,287,034.489(51)	153	0(1)	106	4,636,336.821(224)	−554	0(1)
42	2,340,773.242(38)	60	−60(5)	107	4,637,408.255(53)	−411	0(9)
43	2,353,116.027(38)	−74	76(7)	108	4,639,564.820(71)	1211	0(1)
44	2,389,898.207(38)	−152	−46(5)	109	4,713,837.243(214)	194	0(4)
45	2,406,767.120(38)	177	0(9)	110	4,723,224.243(85)	144	−41(8)
46	2,437,474.985(59)	201	0(1)	111	4,757,672.856(46)	−110	0(9)
47	2,439,319.592(38)	−15	20(6)	112	4,793,077.382(64)	−178	0(1)
48	2,609,740.484(36)	−30	0(6)	113	4,813,320.420(69)	308	179(5)
49	2,612,984.953(51)	−70	−8(8)	114	4,850,055.006(44)	338	0(9)
50	2,621,117.184(39)	169	12(8)	115	4,972,521.517(99)	138	ORP
51	2,631,176.821(46)	223	38(5)	116	4,977,140.283(53)	−81	19(7)
52	2,675,583.371(39)	−155	−14(6)	117	5,003,094.161(59)	33	−21(7)
53	2,756,841.024(39)	−133	−82(4)	118	5,077,587.318(90)	−199	−7(5)
54	2,842,780.905(42)	−190	2(7)	119	5,188,886.526(39)	36	9(7)
55	2,861,900.086(36)	34	−27(7)	120	5,191,688.836(44)	183	111(5)
56	2,886,328.247(36)	29	4(6)	121	5,264,693.665(42)	−417	0(8)
57	2,952,957.663(38)	−67	−75(4)	122	5,268,608.573(48)	113	0(8)
58	2,981,148.445(36)	−150	−84(6)	123	5,294,347.567(42)	39	FSN1
59	2,991,364.726(36)	−102	15(6)	124	5,297,156.277(56)	186	15(5)
60	3,008,619.064(39)	−116	20(6)	125	5,306,809.792(90)	−394	0(4)
61	3,009,824.350(71)	185	31(8)	126	5,307,776.850(51)	−11	FSN2
62	3,089,686.890(38)	76	0(6)	127	5,310,760.945(156)	627	0(6)
63	3,125,616.717(36)	105	−20(5)				
64	3,129,925.963(42)	60	−7(6)				
65	3,147,209.261(36)	−144	−15(6)				

<sup>a</sup>FSN = floating spectroscopic network, ORP = orphan (see Ref. [9] and the text for more details).

Table 5

Measured and calculated H<sub>2</sub><sup>18</sup>O transitions<sup>a</sup>

No.	Frequency (MHz)	Obs–Calc. (kHz)		No.	Frequency (MHz)	Obs–Calc. (kHz)	
		Watsonian	MARVEL			Watsonian	MARVEL
1	5625.147(30)	9	−23(4)	65	3,017,158.833(36)	−71	17(6)
2	<b>203,407.502(30)</b>	<b>253</b>	<b>−12(4)</b>	66	3,019,734.029(38)	−240	−6(7)
3	<b>322,465.170(30)</b>	<b>24</b>	<b>11(5)</b>	67	3,056,987.150(42)	363	86(5)
4	390,607.760(30)	8	8(4)	68	3,098,412.349(38)	79	−24(4)
5	489,054.260(30)	59	−6(3)	<b>69</b>	<b>3,116,280.544(38)</b>	<b>−340</b>	<b>−13(6)</b>
6	<b>517,181.960(30)</b>	<b>49</b>	<b>−13(6)</b>	70	3,117,293.330(38)	201	−42(5)
7	520,137.320(30)	372	−49(5)	71	3,150,956.912(38)	69	1(4)
8	537,337.570(30)	−84	31(6)	72	3,167,316.921(46)	−211	85(5)
9	547,676.440(30)	−108	23(2)	<b>73</b>	<b>3,182,712.688(36)</b>	<b>225</b>	<b>7(6)</b>
10	554,859.748(60)	101	−23(6)	<b>74</b>	<b>3,271,757.942(38)</b>	<b>111</b>	<b>0(7)</b>
11	692,079.347(36)	−541	−22(4)	<b>75</b>	<b>3,296,734.387(39)</b>	<b>−34</b>	<b>8(4)</b>

Table 5 (continued)

No.	Frequency (MHz)	Obs–Calc. (kHz)		No.	Frequency (MHz)	Obs–Calc. (kHz)	
		Watsonian	MARVEL			Watsonian	MARVEL
12	<b>745,320.142(36)</b>	<b>128</b>	−6(4)	76	3,400,030.853(39)	10	FSN1
13	<b>970,276.659(36)</b>	<b>−130</b>	<b>11(5)</b>	77	3,445,526.204(36)	820	0(8)
14	994,674.431(36)	170	41(3)	78	3,535,045.216(38)	−42	11(5)
15	1,095,628.955(36)	308	28(3)	<b>79</b>	<b>3,586,431.043(44)</b>	<b>−355</b>	<b>−8(5)</b>
16	1,101,697.036(36)	−158	0(2)	80	3,591,263.266(56)	76	0(7)
17	1,136,703.041(36)	−18	51(3)	81	3,620,500.441(42)	−295	FSN2
18	1,181,396.004(36)	329	10(3)	82	3,636,466.380(44)	294	57(4)
19	1,188,864.647(36)	99	44(5)	83	3,675,795.023(39)	−164	72(6)
20	<b>1,199,004.040(36)</b>	<b>−291</b>	<b>−12(4)</b>	84	3,696,249.232(38)	334	FSN3
21	1,216,849.584(36)	471	21(5)	85	3,700,536.122(93)	−500	0(13)
22	1,252,570.303(39)	−232	0(7)	86	3,760,381.332(39)	−124	0(7)
23	<b>1,270,059.914(36)</b>	<b>−645</b>	<b>10(6)</b>	87	3,762,496.201(64)	1039	0(7)
24	1,340,733.590(36)	417	23(4)	88	3,769,506.447(46)	28	−7(3)
25	1,367,758.352(36)	−334	−16(6)	89	3,807,723.582(277)	−414	83(6)
26	1,402,970.791(36)	103	−25(4)	90	3,864,028.946(36)	−351	−85(5)
27	1,438,635.938(38)	68	−36(6)	91	3,868,621.212(38)	497	−18(6)
28	1,605,963.652(36)	217	41(5)	92	3,870,153.180(39)	346	0(7)
29	<b>1,620,855.257(42)</b>	<b>−170</b>	<b>−5(6)</b>	93	3,871,373.851(46)	−455	−13(6)
30	1,633,482.650(36)	−180	−22(3)	94	3,889,278.593(38)	−941	0(8)
31	1,655,865.959(36)	−170	−35(2)	95	4,022,058.648(277)	−1130	FSN4
32	1,656,197.895(42)	297	−30(4)	96	4,049,304.037(103)	−12	40(5)
33	1,719,249.729(36)	−130	−10(3)	97	4,055,475.586(39)	−859	FSN3
34	<b>1,719,976.985(36)</b>	<b>−421</b>	<b>−18(6)</b>	98	4,150,075.460(46)	−134	0(5)
35	1,771,672.189(36)	−117	28(5)	99	4,154,598.933(77)	93	−76(7)
36	<b>1,800,483.386(36)</b>	<b>115</b>	<b>−16(6)</b>	<b>100</b>	<b>4,171,320.223(64)</b>	<b>100</b>	<b>18(6)</b>
37	1,815,848.526(36)	−283	12(4)	101	4,178,056.034(51)	175	−57(5)
38	1,815,970.280(36)	1	−2(6)	102	4,224,538.935(103)	−977	−90(7)
39	<b>1,894,322.824(36)</b>	<b>474</b>	<b>11(4)</b>	103	4,376,081.039(46)	175	−76(3)
40	1,974,643.232(36)	−117	4(4)	104	4,416,284.094(44)	278	−54(4)
41	1,985,915.025(35)	−208	55(5)	105	4,461,848.181(51)	288	−1(3)
42	<b>2,099,965.844(36)</b>	<b>−123</b>	<b>−22(4)</b>	106	4,510,186.958(64)	139	FSN1
43	2,143,749.226(36)	68	28(3)	107	4,534,163.808(75)	−201	54(5)
44	2,147,731.770(36)	159	56(4)	108	4,557,466.890(51)	491	FSN4
45	2,227,870.337(36)	77	0(4)	109	4,559,552.927(65)	257	30(4)
46	2,242,195.713(39)	105	0(4)	110	4,564,558.314(99)	−292	FSN2
47	2,318,553.879(36)	153	58(4)	111	4,590,355.444(680)	603	0(3)
48	2,361,122.444(36)	212	22(5)	112	4,585,976.470(114)	−1692	0(10)
49	<b>2,388,325.067(36)</b>	<b>−288</b>	<b>−1(4)</b>	113	4,588,605.610(149)	1264	0(11)
50	2,418,469.036(36)	−213	1(4)	114	4,589,221.268(99)	962	0(9)
51	2,446,246.202(38)	−110	0(12)	115	4,592,194.400(625)	−588	0(3)
52	2,582,720.292(36)	114	16(6)	116	4,704,517.673(39)	71	0(34)
53	<b>2,591,048.043(36)</b>	<b>−319</b>	<b>−41(5)</b>	117	4,713,360.504(133)	60	−16(6)
54	2,622,939.667(42)	209	−2(3)	118	4,751,869.061(194)	1538	−164(7)
55	2,653,659.320(44)	96	−1(5)	<b>119</b>	<b>4,780,743.158(107)</b>	<b>−57</b>	<b>0(7)</b>
56	<b>2,666,726.307(59)</b>	<b>142</b>	<b>−23(5)</b>	120	4,785,166.445(44)	23	FSN3
57	2,741,672.285(36)	−126	35(2)	121	48,91,457.231(107)	276	0(10)
58	<b>2,805,378.378(36)</b>	<b>−148</b>	<b>6(6)</b>	<b>122</b>	<b>4,959,096.406(80)</b>	<b>−140</b>	<b>28(6)</b>
59	2,845,982.199(36)	7	20(5)	123	5,020,343.166(123)	104	63(7)
60	2,888,018.719(77)	−44	−58(6)	124	5,051,272.514(80)	−95	14(4)
61	2,938,998.549(36)	−56	−41(3)	125	5,183,153.399(110)	61	117(4)
62	2,969,866.143(38)	−109	−40(5)	<b>126</b>	<b>5,183,321.763(48)</b>	<b>508</b>	<b>14(6)</b>
63	2,990,141.426(44)	−484	−21(4)	127	5,240,714.945(62)	−19	0(2)
64	3,004,466.833(36)	−426	10(4)				

<sup>a</sup>FSN = floating spectroscopic network, ORP = orphan (see Ref. [9] and the text for more details). Recommended frequency standards are indicated in bold face.

Table 6

Measured and calculated D<sub>2</sub><sup>16</sup>O transitions<sup>a</sup>

No.	Frequency (MHz)	Obs-Calc. (kHz)		No.	Frequency (MHz)	Obs-Calc. (kHz)	
		Watsonian	MARVEL			Watsonian	MARVEL
1	<b>10,919.41</b>	-27	-9(4)	96	1,858,089.610(41)	-6	28(5)
2	10,947.18	99	60(3)	97	1,862,114.253(45)	4	34(4)
3	30,182.49	-139	0(6)	98	1,867,070.394(171)	186	157(5)
4	30,778.50	-116	0(8)	<b>99</b>	<b>1,891,829.820(36)</b>	<b>30</b>	<b>12(5)</b>
5	43,414.56	32	12(3)	100	1,903,352.073(36)	38	3(4)
6	55,482.32	-88	-103(5)	<b>101</b>	<b>1,903,660.786(59)</b>	-1	-3(5)
7	70,240.63	-67	-7(5)	102	1,904,922.080(37)	-12	13(5)
8	<b>74,471.69</b>	<b>-42</b>	<b>-5(6)</b>	103	1,913,971.246(55)	18	7(4)
9	93,350.06	-117	-127(4)	104	1,915,511.368(88)	-58	-36(4)
10	<b>104,875.71</b>	<b>20</b>	<b>2(5)</b>	105	1,920,687.354(39)	-4	0(4)
11	151,710.40	-11	11(3)	106	1,931,792.769(54)	59	0(4)
12	<b>180,171.22</b>	<b>71</b>	<b>20(5)</b>	<b>107</b>	<b>1,943,341.484(37)</b>	<b>-24</b>	<b>2(5)</b>
13	181,833.02	-166	-104(5)	108	1,996,904.485(36)	25	-11(4)
14	187,633.10	-155	-58(4)	<b>109</b>	<b>2,011,053.447(44)</b>	<b>-12</b>	<b>13(5)</b>
15	<b>192,519.44</b>	<b>-78</b>	<b>0(5)</b>	110	2,072,754.810(39)	-21	18(3)
16	218,442.50	29	2(4)	<b>111</b>	<b>2,092,680.133(41)</b>	<b>25</b>	<b>1(5)</b>
17	227,010.50	-136	-102(4)	112	2,104,010.651(42)	67	-1(3)
18	307,107.53	-12	15(5)	113	2,170,174.279(41)	-146	-125(4)
19	307,743.14	3	-36(4)	114	2,177,194.243(41)	-66	-77(4)
20	308,133.65	227	37(6)	115	2,277,013.478(38)	33	26(4)
21	316,799.81	-21	-15(2)	116	2,293,369.151(44)	-34	-16(5)
22	339,035.26	163	149(5)	<b>117</b>	<b>2,330,851.127(38)</b>	<b>18</b>	<b>16(6)</b>
23	393,332.82	79	26(4)	<b>118</b>	<b>2,333,887.400(36)</b>	<b>16</b>	<b>31(5)</b>
24	403,251.62	-24	-14(7)	119	2,376,878.544(40)	-33	-2(4)
25	403,377.36	12	-14(6)	120	2,397,641.676(41)	-47	-12(5)
26	403,561.82	-145	-72(4)	<b>121</b>	<b>2,400,382.322(40)</b>	<b>13</b>	<b>-2(5)</b>
27	<b>430,949.26</b>	<b>-1</b>	<b>37(5)</b>	<b>122</b>	<b>2,401,599.350(38)</b>	<b>15</b>	<b>29(5)</b>
28	458,531.45	106	24(3)	123	2,407,649.965(37)	40	-4(4)
29	<b>468,246.57</b>	<b>58</b>	<b>-24(3)</b>	124	2,410,887.788(38)	-30	51(4)
30	469,619.170	-10	ORP1	125	2,412,421.601(51)	5	-61(5)
31	469,633.530	8	ORP2	<b>126</b>	<b>2,465,848.800(120)</b>	<b>-16</b>	<b>-16(5)</b>
32	555,330.278(37)	33	34(3)	127	2,472,191.939(39)	68	54(4)
33	571,220.050(40)	14	-11(4)	128	2,477,700.224(36)	1	-4(4)
34	572,114.814(36)	10	0(4)	129	2,487,871.584(58)	-63	-86(3)
35	607,349.439(36)	36	0(2)	130	2,492,960.465(37)	32	2(4)
36	<b>643,247.288(37)</b>	<b>5</b>	<b>14(5)</b>	131	2,528,196.099(44)	-72	-57(4)
37	649,560.254(41)	-65	-28(5)	132	2,584,670.452(36)	-96	-36(3)
38	<b>692,243.579(36)</b>	<b>32</b>	<b>-32(4)</b>	133	2,654,868.110(67)	-26	-49(5)
39	697922.831(36)	62	75(3)	<b>134</b>	<b>2,688,283.075(71)</b>	<b>5</b>	<b>7(4)</b>
40	<b>714,087.313(36)</b>	<b>32</b>	<b>21(5)</b>	<b>135</b>	<b>2,689,181.271(37)</b>	<b>-30</b>	<b>-4(5)</b>
41	722,669.979(36)	26	30(3)	136	2,736,804.981(38)	-3	18(4)
42	740,648.830(54)	-45	17(4)	137	2,807,098.229(92)	-65	-54(3)
43	<b>743,563.526(36)</b>	<b>38</b>	<b>-8(4)</b>	138	2,885,276.612(180)	-7	47(4)
44	751,110.615(36)	-13	-33(4)	139	2,889,555.699(56)	-45	-56(6)
45	<b>782,470.894(36)</b>	<b>-3</b>	<b>-13(4)</b>	140	2,893,642.415(45)	-10	-33(5)
46	850,757.646(36)	77	-6(3)	141	2,898,621.125(42)	62	13(5)
47	<b>890,396.169(36)</b>	<b>-35</b>	<b>-25(5)</b>	142	2,899,555.915(37)	31	43(4)
48	897,947.107(36)	-17	22(2)	143	2,899,626.742(73)	81	52(6)
49	922,666.552(54)	106	26(4)	144	2,902,252.230(49)	-46	-143(6)
50	<b>930,942.494(36)</b>	<b>-38</b>	<b>-16(4)</b>	145	2,902,428.470(65)	-120	-89(4)
51	947,556.517(42)	47	47(3)	146	2,997,072.252(44)	70	84(4)
52	951,194.083(38)	-70	-28(4)	147	3,098,437.767(37)	-91	-63(5)
53	<b>1,025,247.592(75)</b>	<b>-4</b>	<b>40(5)</b>	148	3,324,671.327(71)	141	131(3)
54	1,043,212.727(36)	35	15(4)	149	3,339,592.524(36)	136	129(4)
55	<b>1,049,534.487(40)</b>	<b>23</b>	<b>18(5)</b>	150	3,367,260.520(59)	50	62(5)

Table 6 (continued)

No.	Frequency (MHz)	Obs–Calc. (kHz)		No.	Frequency (MHz)	Obs–Calc. (kHz)	
		Watsonian	MARVEL			Watsonian	MARVEL
56	<b>1,065,096.951(36)</b>	<b>25</b>	<b>3(4)</b>	151	3,367,279.110(40)	-10	26(6)
57	<b>1,074,239.946(36)</b>	<b>-23</b>	<b>7(5)</b>	152	3,367,685.512(59)	33	0(7)
58	1,076,067.817(36)	32	12(4)	153	3,367,809.159(40)	0	0(6)
59	1,076,226.486(36)	-67	-33(4)	154	3,378,057.828(38)	-7	-15(3)
60	<b>1,084,697.772(36)</b>	<b>-45</b>	<b>-17(5)</b>	155	3,379,032.803(38)	8	-61(3)
61	1,104,667.270(39)	42	52(4)	156	3,380,930.919(49)	17	64(4)
62	1,115,694.317(36)	0	-29(4)	<b>157</b>	<b>3,385,405.730(59)</b>	<b>-87</b>	<b>-29(5)</b>
63	1,158,044.885(36)	-5	40(4)	<b>158</b>	<b>3,535,559.341(120)</b>	<b>20</b>	<b>32(5)</b>
64	1,169,734.995(36)	-6	-6(4)	<b>159</b>	<b>3,619,317.293(47)</b>	<b>-31</b>	<b>-18(4)</b>
65	<b>1,174,586.218(36)</b>	<b>23</b>	<b>17(5)</b>	160	3,697,832.834(97)	39	69(4)
66	<b>1,213,568.563(36)</b>	<b>2</b>	<b>12(4)</b>	161	3,741,269.401(38)	-72	-51(5)
67	1,223,121.625(36)	-26	-23(3)	162	3,754,519.171(37)	-32	2(4)
68	1,236,240.541(40)	-22	8(4)	163	3,776,395.270(38)	64	49(5)
69	<b>1,247,703.885(37)</b>	<b>13</b>	<b>-30(4)</b>	164	3,782,959.825(64)	-53	-43(4)
70	<b>1,251,173.516(54)</b>	<b>-20</b>	<b>15(5)</b>	165	3,833,183.610(50)	-27	46(5)
71	1,262,090.454(36)	-22	9(4)	166	3,846,163.892(59)	15	28(5)
72	1,331,417.531(36)	-3	43(3)	167	3,862,332.991(36)	32	-9(4)
73	<b>1,396,175.485(38)</b>	<b>-22</b>	<b>-33(4)</b>	168	3,914,245.631(61)	-26	-104(4)
74	1,403,825.537(36)	-20	-10(3)	169	4,060,351.346(109)	38	63(3)
75	1,404,963.376(41)	-49	-13(3)	170	4,070,094.342(88)	128	195(6)
76	1,410,311.882(225)	86	105(5)	171	4,085,368.747(52)	-65	-51(4)
77	1,415,793.386(36)	-85	-53(5)	<b>172</b>	<b>4,137,172.519(62)</b>	<b>-19</b>	<b>-10(5)</b>
78	1,419,292.416(40)	28	-16(5)	<b>173</b>	<b>4,261,861.286(52)</b>	<b>7</b>	<b>-20(5)</b>
79	1,432,266.246(36)	14	0(3)	174	4,262,055.007(90)	21	171(4)
80	<b>1,464,785.824(36)</b>	<b>-21</b>	<b>-2(5)</b>	175	4,394,203.184(120)	171	181(5)
81	<b>1,497,312.256(37)</b>	<b>-28</b>	<b>-19(5)</b>	176	4,435,920.495(95)	41	-15(4)
82	1,528,703.708(36)	-55	-22(2)	177	4,582,713.451(58)	-97	-59(5)
83	<b>1,544,144.781(40)</b>	<b>22</b>	<b>21(5)</b>	178	4,630,904.565(36)	77	16(4)
84	1,550,720.750(37)	95	75(3)	179	4,632,632.725(45)	-31	-61(5)
85	<b>1,580,060.751(38)</b>	<b>-23</b>	<b>-18(5)</b>	180	4,651,524.577(56)	14	28(4)
86	1,597,742.538(38)	-44	-43(4)	181	4,821,526.699(106)	-65	-75(5)
87	1,615,372.081(43)	116	61(3)	182	4,985,151.759(48)	-93	-60(6)
88	1,648,499.608(43)	-20	-20(4)	<b>183</b>	<b>4,988,188.093(171)</b>	<b>-34</b>	<b>16(5)</b>
89	16,56,547.715(40)	-21	73(5)	184	4,994,501.210(49)	48	125(5)
90	1,703,425.922(37)	-28	-20(4)	185	5,002,971.123(63)	150	110(4)
91	1,736,774.264(36)	40	36(5)	186	5,122,445.287(450)	26	-84(5)
92	1,755,338.658(36)	10	-18(4)	187	5,122,463.195(189)	-241	-303(5)
93	1,794,965.199(42)	20	-18(4)	188	5,144,901.449(225)	-128	-88(5)
94	1,801,301.264(86)	78	25(5)				
95	1,819,579.805(36)	-47	-96(4)				

<sup>a</sup> Recommended frequency standards are indicated in bold face.

(serial number: 5), which have a considerable effect on all higher transitions. It is also clear that most levels are determined by a large number of transitions.

### 3.4. Connecting with the region 0–15 cm<sup>-1</sup>

The MARVEL energy levels obtained from measurement in the 15–170 cm<sup>-1</sup> window can be used to make predictions for transitions between 0 and 15 cm<sup>-1</sup>. These transitions have previously been measured with high accuracy by microwave and millimeterwave spectroscopies [22–27]. Furthermore, for the H<sub>2</sub><sup>17</sup>O isotopologue a previous full MARVEL analysis of the levels and lines is available [9], providing data for an even more elaborate comparison.

Table 7

Measured and calculated H<sub>2</sub><sup>16</sup>O v<sub>2</sub> = 1 transitions<sup>a</sup>

No.	Frequency (MHz)	Obs–Calc. (kHz)		No.	Frequency (MHz)	Obs–Calc. (kHz)	
		Watsonian	MARVEL			Watsonian	MARVEL
1	<b>2159.980(30)</b>	<b>−1265</b>	<b>1(23)</b>	66	2,586,380.192(101)	374	0(3)
2	12,008.800(30)	−394	−38(14)	67	2,590,792.169(48)	−62	72(14)
3	26,834.270(30)	207	−4(17)	68	2,646,587.259(345)	920	57(14)
4	67,803.960(40)	658	17(14)	69	2,689,142.154(141)	1533	366(14)
5	96,261.160(100)	−946	−45(25)	70	2,742,473.460(147)	853	FSN2
<b>6</b>	<b>119,995.940(100)</b>	<b>120</b>	<b>28(21)</b>	71	2,783,474.132(196)	708	239(15)
7	209,118.370(100)	−273	0(31)	72	2,807,970.677(212)	970	5(24)
8	232,686.700(998)	−174	−83(20)	73	2,820,924.448(66)	−113	0(3)
9	262,897.748(100)	94	ORP1	74	2,842,959.455(130)	−654	FSN2
10	263,451.357(100)	−94	ORP2	75	2,901,971.494(130)	139	−62(15)
11	293,664.442(100)	−72	0(24)	76	2,973,033.665(132)	−611	−10(15)
12	297,439.107(100)	12	0(31)	77	3,024,919.504(50)	−137	−29(30)
13	323,554.019(100)	1	ORP3	78	3,036,348.362(63)	230	−7(30)
14	336,227.620(200)	−1644	−306(17)	79	3,037,604.656(93)	−709	−37(23)
15	425,689.190(100)	−101	0(23)	80	3,051,881.612(41)	−45	11(14)
16	438,724.178(100)	867	ORP4	81	3,065,529.852(85)	144	−97(24)
17	440,736.910(100)	482	ORP5	82	3,113,657.661(133)	964	FSN1
18	441,238.866(100)	−930	ORP6	83	3,132,327.598(73)	880	32(28)
19	463,170.460(1000)	−1034	120(25)	84	3,159,149.351(139)	1910	58(22)
20	498,502.590(100)	−474	112(30)	85	3,161,575.971(129)	213	0(3)
21	546,690.600(1000)	635	603(24)	<b>86</b>	<b>3,253,325.223(58)</b>	<b>−421</b>	<b>−9(20)</b>
22	548,474.403(100)	4	ORP7	87	3,275,649.015(59)	458	−12(21)
23	578,057.486(100)	−58	36(22)	88	3,310,494.131(64)	451	−14(17)
24	593,708.497(100)	−206	0(30)	89	3,472,884.552(36)	35	ORP8
25	595,079.800(1000)	1051	50(18)	90	3,494,856.711(196)	550	328(29)
26	658,006.500(100)	947	298(9)	91	3,553,520.949(41)	−663	12(17)
27	859,965.415(337)	831	−5(22)	92	3,566,075.653(142)	−854	423(25)
28	899,302.169(158)	−948	75(20)	93	3,623,901.000(127)	−664	−57(18)
29	902,609.434(36)	240	17(14)	94	3,638,527.595(81)	−111	1(17)
30	923,113.205(90)	430	5(17)	95	3,639,917.297(83)	856	−24(29)
31	926,187.475(253)	−408	−316(28)	96	3,660,797.831(269)	−29	−251(25)
32	968,047.110(98)	−63	1(21)	97	3,708,481.609(187)	−170	447(26)
33	1,077,763.094(90)	45	−29(28)	98	3,718,431.227(72)	−474	FSN2
34	1,205,788.836(257)	−35	0(14)	99	3,740,915.533(166)	−801	−167(17)
35	1,214,662.173(57)	1316	109(14)	100	3,756,027.296(192)	−747	−129(27)
36	1,215,068.547(256)	14	25(22)	101	3,782,897.903(36)	−33	FSN2
37	1,222,823.933(185)	604	−127(30)	102	3,869,939.727(75)	64	−19(17)
38	1,406,675.828(44)	−633	47(14)	103	3,883,916.886(101)	−428	−2(2)
39	1,421,957.809(188)	−605	170(22)	104	3,906,840.512(65)	−813	0(4)
40	1,428,471.583(72)	674	348(30)	105	4,007,106.580(177)	1289	FSN1
41	1,473,570.178(91)	−645	16(16)	106	4,032,353.881(44)	−318	−1(2)
42	1,494,057.717(170)	−226	−1(22)	107	4,048,000.053(63)	304	1(2)
43	1,592,067.968(110)	−787	142(16)	108	4,065,271.976(90)	−18	156(14)
44	1,643,919.389(42)	−689	104(14)	109	4,120,648.634(181)	−1111	0(3)
<b>45</b>	<b>1,739,351.616(162)</b>	<b>1343</b>	<b>−17(21)</b>	110	<b>4,133,825.463(74)</b>	<b>−853</b>	<b>−18(17)</b>
46	1,740,398.130(91)	−236	−4(21)	111	4,196,284.856(340)	130	−5(22)
47	1,753,915.504(102)	37	−366(10)	112	4,253,823.554(47)	−313	0(2)
<b>48</b>	<b>1,849,183.362(72)</b>	<b>574</b>	<b>−11(21)</b>	113	<b>4,265,257.100(65)</b>	<b>−297</b>	<b>−25(14)</b>
49	1,933,475.376(245)	−340	−395(21)	114	4,265,437.327(95)	1154	0(3)
50	1,946,459.921(199)	−416	250(27)	115	4,450,244.299(36)	−68	8(17)
51	1,955,971.792(36)	50	−140(14)	116	4,457,402.217(111)	−316	−136(22)
52	2,090,772.849(134)	−1077	0(3)	117	4,551,455.354(103)	975	ORP8
53	2,107,023.195(146)	−210	−2(19)	118	4,557,683.503(151)	−529	9(22)
<b>54</b>	<b>2,140,487.424(81)</b>	<b>−13</b>	<b>17(27)</b>	119	<b>4,583,551.948(228)</b>	<b>944</b>	<b>0(4)</b>
<b>55</b>	<b>2,227,574.508(36)</b>	<b>−7</b>	<b>−2(21)</b>	120	<b>4,608,238.672(114)</b>	1094	<b>200(31)</b>

Table 7 (continued)

No.	Frequency (MHz)	Obs–Calc. (kHz)		No.	Frequency (MHz)	Obs–Calc. (kHz)	
		Watsonian	MARVEL			Watsonian	MARVEL
56	<b>2,234,027.230(36)</b>	<b>523</b>	<b>3(21)</b>	121	4,625,215.016(36)	41	0(8)
57	<b>2,247,746.378(36)</b>	<b>−253</b>	<b>−8(30)</b>	122	4,631,067.359(57)	630	11(22)
58	2,294,179.819(40)	246	8(17)	123	4,632,796.724(59)	−140	59(30)
59	<b>2,337,406.253(37)</b>	<b>−777</b>	<b>3(21)</b>	124	4,644,850.822(57)	−109	0(22)
60	2,372,358.488(61)	133	0(22)	125	4,654,349.333(159)	848	FSN1
61	<b>2,401,232.308(48)</b>	<b>930</b>	<b>−3(16)</b>	126	4,672,518.687(103)	−127	−181(29)
62	2,484,150.917(45)	−60	6(17)	127	4,681,341.330(184)	352	0(4)
63	2,488,754.824(127)	670	109(24)	128	4,707,457.308(67)	118	0(8)
64	2,519,730.252(525)	943	276(16)	129	4,809,360.758(117)	−345	−77(17)
65	2,541,727.798(180)	−691	−11(26)	130	4,955,872.295(36)	301	−103(14)

<sup>a</sup>FSN = floating spectroscopic network, ORP = orphan (see Ref. [9] and the text for more details). Recommended frequency standards are indicated in bold face.

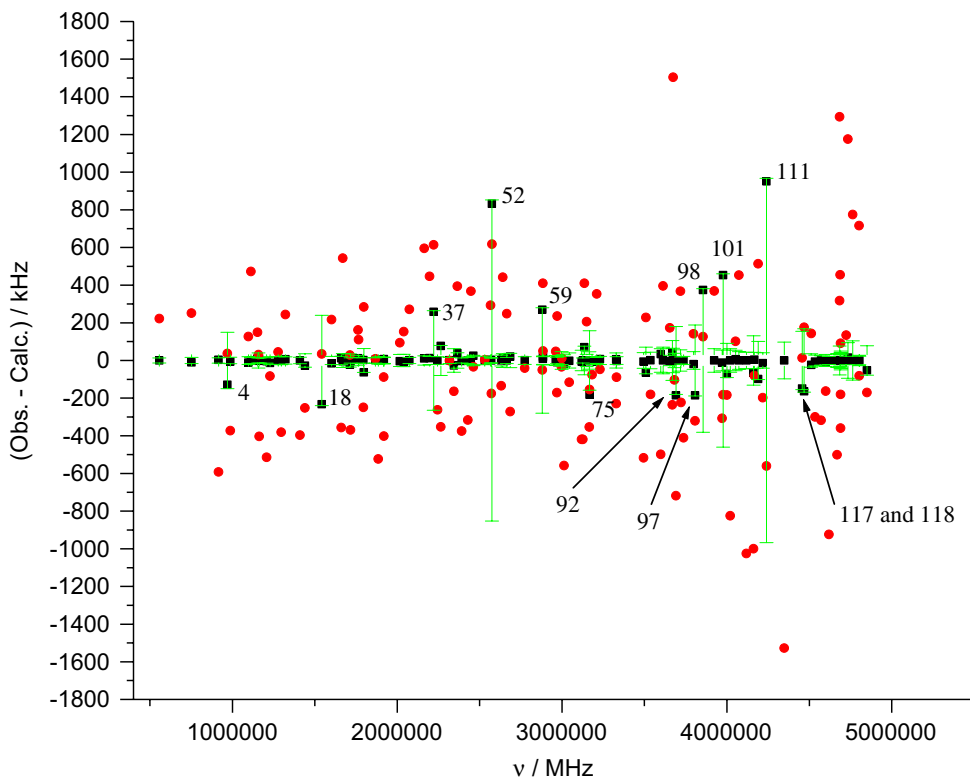


Fig. 2. Reproduction of the measured pure rotational transitions of  $\text{H}_2^{16}\text{O}$  by the  $A$ -reduced Watsonian (●) and the MARVEL (■) approaches. The uncertainties indicated were determined by MARVEL through the robust reweighting protocol with  $\alpha = 0.01$ . The numbered uncertainties, where the number given corresponds to the serial number of the transition given in Table 3, denote those instances where MARVEL increased the original experimental uncertainties significantly.

As detailed in Table 9, these comparisons can be performed only for a small number of transitions. Nevertheless, the considerable precision of the MARVEL rotational energy levels based on the measurements of Matsushima et al. is confirmed. These comparisons also suggest that the measurement uncertainties suggested by Matsushima et al., about 200–400 kHz ( $2\sigma$ ), appear to be more reliable than the smaller internal inaccuracies suggested by MARVEL. The only outstandingly large discrepancies observed, those above 400 kHz, concern the  $5_{33}–4_{40}$  transition for  $\text{H}_2^{16}\text{O}$ , and the  $6_{42}–5_{51}$  and  $7_{53}–6_{60}$  transitions for  $\text{D}_2^{16}\text{O}$ . The only common feature of these problematic transitions is that they all involve a  $J = K_a$  rotational level. The observed inaccuracies require further studies and perhaps new, ever more accurate measurements.

Table 8

Selected elements, with a cut-off value of 0.25, of the computed sensitivity matrix  $\mathbf{S}$  for the  $J = 2\text{--}4$  SN1 energy levels of  $\text{H}_2^{16}\text{O}^{\text{a}}$ 

$J K_a K_c$	Sensitivity matrix element
2 0 2	0.67(5) -0.26(12) 0.33(63)
2 1 1	0.43(2) 0.51(5) -0.45(12) 0.49(63)
2 2 0	0.33(5) 0.26(12) 0.67(63)
3 1 3	0.56(5) -0.34(31) 0.50(35) 0.44(63) 0.29(82)
3 2 2	0.52(5) 0.31(31) 0.35(35) 0.48(63) 0.42(82)
3 3 1	-0.29(3) 0.48(5) 0.30(35) 0.29(43) 0.52(63) 0.28(82) 0.42(118)
4 0 4	0.54(5) -0.29(19) 0.44(35) 0.59(44) 0.46(63) 0.31(82)
4 1 3	0.29(3) 0.52(5) -0.30(11) 0.26(19) 0.41(34) 0.38(35) 0.30(44) 0.48(63) 0.34(82) 0.28(118)
4 2 2	0.48(3) 0.50(5) 0.41(11) 0.26(34) 0.35(35) 0.26(44) 0.50(63) 0.31(82) 0.34(118)
4 3 1	0.37(3) -0.31(4) 0.52(5) 0.52(33) 0.38(35) 0.39(44) 0.48(63) 0.31(82) 0.30(118)
4 4 0	0.37(3) -0.31(4) 0.52(5) 0.52(33) 0.38(35) 0.39(44) 0.48(63) 0.31(82) 0.30(118)

<sup>a</sup>Numbers in parentheses show the serial number, taken from Table 3, of the transition having a sensitivity coefficient larger than 0.25 for the rotational level  $J K_a K_c$  (Table 1). Transition 7, which has a sensitivity coefficient 1 for all the levels, has not been included in the table. The number of coefficients increases further with increase in  $J$ .

Table 9

Comparison of directly measured transitions in the 0–15 cm<sup>−1</sup> window to those based on MARVEL levels determined from transitions in the 15–170 cm<sup>−1</sup> window within this study

Isotopologue	$J' K'_a K'_c - J'' K''_a K''_c$	Measured frequency (MHz)	This work (MHz)	Diff (kHz)
$\text{H}_2^{16}\text{O}$	3 1 3–2 2 0	183,310.0906(15) [22]	183,310.0728	18
		183,310.117(2) [23]		44
		183,310.075(5) [24]		2
	5 1 5–4 2 2	325,152.919(150) [23]	325,152.9699	-51
	5 3 3–4 4 0	474,689.127(150) [23]	474,689.5588	-432
$\text{H}_2^{17}\text{O}$	6 2 4–7 1 7	488,491.133(150) [23]	488,491.1421	-9
	3 1 3–2 2 0	194,002.322(3) [25]	194,002.2920	30
		194,002.322(2) [9]		30
	5 1 5–4 2 2	323,826.534(5) [25]	323,826.2650	269
$\text{H}_2^{18}\text{O}$		323,826.325(3) [9]		60
	3 1 3–2 2 0	203,407.52(2) [26]	203,407.5144	6
	5 1 5–4 2 2	322,465.17(5) [26]	322,465.1592	11
$\text{D}_2^{16}\text{O}$	3 1 3–2 2 0	10,919.39(33) [27]	10,919.4202	-30
	8 7 1–9 6 4	30,778.62(190) [27]	30,778.4998	120
	4 4 0–5 3 3	55,482.32(43) [27]	55,482.4241	-104
	8 5 3–7 6 2	74,471.71(92) [27]	74,471.6948	15
	6 2 4–7 1 7	104,875.80(67) [27]	104,875.7088	91
	5 5 1–6 4 2	180,170.11(67) [27]	180,171.2003	-1090
	5 1 5–4 2 2	181,832.90(41) [27]	181,833.1240	-224
	7 4 4–6 5 1	192,519.52(50) [27]	192,519.4406	79
	4 2 2–3 3 1	227,010.52(52) [27]	227,010.6037	-84
	6 6 0–7 5 3	308,133.18(89) [27]	308,133.6117	-432

#### 4. Summary

The protocol MARVEL, standing for measured active rotational–vibrational energy levels, has been employed to check the true internal accuracy of the positions of the pure rotational transitions of the water isotopologues  $\text{H}_2^{16}\text{O}$ ,  $\text{H}_2^{17}\text{O}$ ,  $\text{H}_2^{18}\text{O}$ , and  $\text{D}_2^{16}\text{O}$ , measured by Matsushima and co-workers using a frequency-tunable spectrometer in the far-infrared (FIR) region. The considerable precision of the measurement of the

line positions, on average better than 40 kHz ( $2\sigma$ ) as given by MARVEL, has been confirmed. The line positions appear to be more accurate than claimed in the original papers, where an accuracy of 100–200 kHz ( $1\sigma$ ) was claimed. Nevertheless, when the MARVEL energy levels obtained from the rotational transitions in the 15–170 cm<sup>-1</sup> window are used to predict transitions for the isotopologues in between 0 and 15 cm<sup>-1</sup>, the levels prove to be less accurate than what MARVEL predicted. It seems to be safe to follow Matsushita et al., and suggest employing several of the lines measured by them as frequency standards in the FIR region, more precisely between 15 and 170 cm<sup>-1</sup> (the 0.5–5 THz window). Those lines of H<sub>2</sub><sup>17</sup>O, H<sub>2</sub><sup>18</sup>O, and D<sub>2</sub><sup>16</sup>O are recommended, note that H<sub>2</sub><sup>17</sup>O is excluded due to the quadrupole moment of <sup>17</sup>O and the resulting large splittings, which belong to *para*-water, for which the precision of the measurements, confirmed by MARVEL, is better than 33 kHz ( $2\sigma$ ), and whose underlying energy levels have been involved in at least three measured transitions. For the isotopologues H<sub>2</sub><sup>18</sup>O and D<sub>2</sub><sup>16</sup>O the number of selected rotational transitions on the (000) ground vibrational state is 25 and 46, respectively. For H<sub>2</sub><sup>16</sup>O, the number of selected transitions is 22 for the ground vibrational state and 11 for the (010) bending state.

The protocol MARVEL allowed to test the accuracy of the effective *A*-reduced Watson Hamiltonians for a difficult case, water, under the requirement of extreme accuracy, provided by the measurements of Matsushima et al. The scatter of the line frequency predictions produced by a Watson-type *A*-reduced Hamiltonian with as many as 32 parameters is substantial, in cases more than 1000 kHz but on average several hundred kHz, not only for high but also for low rotational excitations. As proven by MARVEL, the related empirical data have an order of magnitude larger inaccuracy than the measured transitions themselves. This observation questions the use of Watson-type Hamiltonians during such high-accuracy benchmark studies for more than the assignment of the lines. Combined use of Watson-type effective Hamiltonians and MARVEL-type protocols is recommended for high-accuracy spectroscopic studies when the accuracy of the line positions needs to be determined with a high degree of confidence.

The limited amount of transitions data allows the execution of a sensitivity analysis of the MARVEL energy levels, a task that is out of reach for much larger sets of experimental data, more typical of usual spectroscopic applications. It seems that there is no particular advantage the sensitivity analysis can offer for high-accuracy spectroscopic studies, whereby the relation between the experimentally measured transitions and the derived energy levels is linear.

## Acknowledgments

The authors would like to thank Professor Jean Demaison for valuable comments on a draft of the manuscript. This work received support from the Hungarian Scientific Research Fund (OTKA T047185), from the European Union through the MC RTN QUASAAR network, and from the NKTH. This work was performed as part of the activities of the IUPAC Task Group 2004035-1-100.

## References

- [1] Rothman LS, Jacquemart D, Barbe A, Chris Benner D, Birk M, Brown LR, et al. The HITRAN 2004 molecular spectroscopic database. *JQSRT* 2005;96:139–204.
- [2] Jacquinot-Husson N, Scott NA, Chédin A, Garceran K, Armante R, Chursin AA, et al. The 2003 edition of the GEISA/IASI spectroscopic database. *JQSRT* 2005;95:429–67.
- [3] (a) Nielsen HH. The vibration–rotation energies of molecules. *Rev Mod Phys* 1951;23:90–136;
- (b) Aliev MR, Watson JKG. In: Narahari Rao K, editor. Molecular spectroscopy: modern research, vol. III. San Diego, CA: Academic Press; 1985. p. 1–67;
- (c) Bunker PR, Jensen P. Molecular symmetry and spectroscopy. Ottawa: NRC Research Press; 1998.
- [4] (a) Herzberg G. Infrared and Raman spectra of polyatomic molecules. New York: Van Nostrand; 1945;
- (b) Novick SE, Davies P, Harris SJ, Klempner W. Determination of the structure of ArHCl. *J Chem Phys* 1973;59:2273–9.
- [5] Flaud J-M, Camy-Peyret C, Maillard JP. Higher ro-vibrational levels of H<sub>2</sub>O deduced from high resolution oxygen-hydrogen flame spectra between 2800–6200 cm<sup>-1</sup>. *Mol Phys* 1976;32:499–521.
- [6] (a) Watson JKG. On the use of term values in the least-squares fitting of spectra. *J Mol Spectrosc* 1989;138:302–8;
- (b) Watson JKG. The use of term-value fits in testing spectroscopic assignments. *J Mol Spectrosc* 1994;165:283–90.
- [7] Curl RF, Dane CB. Unbiased least-squares fitting of lower states. *J Mol Spectrosc* 1988;128:406–12.

- [8] Åslund N. A numerical method for the simultaneous determination of term values and molecular constants. *J Mol Spectrosc* 1974;50: 424–34.
- [9] Furtenbacher T, Császár AG, Tennyson J. MARVEL: measured active rotational-vibrational energy levels. *J Mol Spectrosc* 2007; 245:115–25.
- [10] Huber PJ. Robust statistics. Hoboken: Wiley; 2004.
- [11] Lin KF, Blass WE, Gailar NM. Ethane spectrum between 1940 and 2152 cm<sup>-1</sup>: ground state parameters. *J Mol Spectrosc* 1980;79: 151–7.
- [12] Watson JKG. Robust weighting in least-squares fits. *J Mol Spectrosc* 2003;219:326–8.
- [13] Ruscic B, Pinzon RE, Morton ML, Von Laszewski G, Bittner SJ, Nijsure SG, et al. Introduction to active thermochemical tables: several key enthalpies of formation revisited. *J Phys Chem A* 2004;108:9979–97.
- [14] Matsushima F, Nagase H, Nakauchi T, Odashima H, Takagi K. Frequency measurement of pure rotational transitions of H<sub>2</sub><sup>17</sup>O and H<sub>2</sub><sup>18</sup>O from 0.5 to 5 THz. *J Mol Spectrosc* 1999;193:217–23.
- [15] Matsushima F, Odashima H, Iwasaki T, Tsunekawa S, Takagi K. Frequency measurement of pure rotational transitions of H<sub>2</sub>O from 0.5 to 5 THz. *J Mol Struct* 1995;352/353:371–8.
- [16] Matsushima F, Matsunaga M, Qian GY, Ohtaki Y, Wang RL, Takagi K. Frequency measurement of pure rotational transitions of D<sub>2</sub>O from 0.5 to 5 THz. *J Mol Spectrosc* 2001;206:41–6.
- [17] Matsushima F, Tomatsu N, Nagai T, Moriwaki Y, Takagi K. Frequency measurement of pure rotational transitions in the v<sub>2</sub> = 1 state of H<sub>2</sub>O. *J Mol Spectrosc* 2006;235:190–5.
- [18] Miani A, Tennyson J. Can ortho–para transitions for water be observed? *J Chem Phys* 2004;120:2732–9.
- [19] Toth RA. Linelists of water vapor parameters from 500 to 8000 cm<sup>-1</sup> <<http://mark4sun.jpl.nasa.gov/data/spec/H2O>>, private communication, 2005.
- [20] Shirin SV, Polyansky OL, Zobov NF, Ovsyannikov RI, Császár AG, Tennyson J. Spectroscopically determined potential energy surfaces of the H<sub>2</sub><sup>16</sup>O, H<sub>2</sub><sup>17</sup>O, and H<sub>2</sub><sup>18</sup>O isotopologues of water. *J Mol Spectrosc* 2006;236:216–23.
- [21] Polyansky OL. One-dimensional approximation of the effective rotational Hamiltonian of the ground state of the water molecule. *J Mol Spectrosc* 1985;112:79–87.
- [22] Huissoon C. A high resolution spectrometer for the shorter millimeter wavelength region. *Rev Sci Instrum* 1971;42(4):477–81.
- [23] De Lucia FC, Helminger P, Cook RL, Gordy W. Submillimeter microwave spectrum of H<sub>2</sub><sup>16</sup>O. *Phys Rev A* 1972;5(2):487–90.
- [24] Golubiatnikov GY. Shifting and broadening parameters of the water vapor 183-GHz line (3<sub>1</sub> 3–2<sub>2</sub> 0) by H<sub>2</sub>O, O<sub>2</sub>, N<sub>2</sub>, CO<sub>2</sub>, H<sub>2</sub>, He, Ne, Ar, and Kr at room temperature. *J Mol Spectrosc* 2005;230:196–8.
- [25] De Lucia FC, Helminger P. Microwave spectrum and ground state energy levels of H<sub>2</sub><sup>17</sup>O. *J Chem Phys* 1975;56:138–45.
- [26] De Lucia FC, Helminger P, Cook RL, Gordy W. Submillimeter microwave spectrum of H<sub>2</sub><sup>18</sup>O. *Phys Rev A* 1972;6(4):1324–6.
- [27] Benedict WS, Clough SA, Frenkel L, Sullivan TE. Microwave spectrum and rotational constants for the ground state of D<sub>2</sub>O. *J Chem Phys* 1970;53:2565–70.